Characterization and crystal structure of (xanthine$^+$)$_2$[ZnCl$_4$]

Gaby Hänggi, Helmut Schmalle and Erich Dubler*
Institute of Inorganic Chemistry, University of Zürich, Winterthurerstrasse 190, CH-8057 Zurich (Switzerland)

(Received February 19, 1992)

Abstract

The reaction of the oxopurine base xanthine with zinc chloride in diluted hydrochloric acid has resulted in the formation of single crystals of the composition (xanthine$^+$)$_2$[ZnCl$_4$]. Crystal data: orthorhombic, space group $Pmn2_1$, $a = 19.701(6)$, $b = 6.583(1)$, $c = 6.610(2)$ Å, $V = 857.3(7)$ Å^3, $Z = 2$, $R = 0.042$ using 1129 observed reflections with $I \geq 3\sigma(I)$. (Xanthine$^+$)$_2$[ZnCl$_4$] contains isolated [ZnCl$_4$]$^{2-}$ tetrahedra and non-coordinating xanthinium cations, which are linked to the anions via strong N–H···Cl hydrogen bonds with donor–acceptor distances in the range 3.202(6)–3.434(6) Å. The discrete xanthinium cations are interconnected by hydrogen bonding contacts of the type N–H···O with N···O distances of 2.782(7) and 2.948(7) Å. A detailed analysis of the alterations of the ring geometry of xanthine upon protonation is given.

Introduction

The importance of crystallographic investigations on the interactions of metals with the nucleobases guanine and adenine, the major purine base present in DNA and RNA, has been widely recognized [1, 2]. In contrast, only a few structural data are available on compounds involving oxopurines such as hypoxanthine and xanthine, which are intermediate products of purine metabolism formed by enzymatical degradation of nucleic acids.

The molybdenum- and iron-containing enzyme xanthine oxidase catalyzes the oxidation of hypoxanthine via xanthine to uric acid [3]. Defects in this metabolism induce precipitation of oxopurines as pathological biogenic solids, observed in conjunction with diseases like gout and xanthinuria. Gout is characterized by an increased level of uric acid, thus leading to deposits of sodium hydrogenurate monohydrate crystals in joints [4]. Crystalline xanthine may be found in muscle tissue as a consequence of the hereditary disease xanthinuria, a rare disorder resulting from a gross deficiency of xanthine oxidase activity [5]. In addition, xanthine occasionally crystallizes as a constituent of urinary calculi [6].

Crystallographic studies on metal complexes of unsubstituted xanthine have elucidated the potential metal binding sites of this purine derivative. In complexes involving neutral xanthine, metalation occurs through the imidazole nitrogen atom N(9) and hydrogen atoms are attached at N(1), N(3) and N(7) [7]. Monodentate coordination has also been established for the monoanion of xanthine in a monomeric cobalt complex [8], where hydrogen atoms are attached at N(1) and N(3). Twofold negatively charged xanthine acts as tridentate ligand coordinating through N(3), N(7) and N(9) to three different methylmercury cations in a complex described by Allaire and Beauchamp [9]. In addition, monodentate N(9) coordination in combination with N(7)/O(6) and N(1)/O(2) chelation of a dianionic xanthine to three different titanocen units is observed in a trinuclear 3:1 titanocene xanthine complex [10]. Finally, complete deprotonation of xanthine increases the number of possible metal binding sites, for example resulting in a polynuclear complex in which four methylmercury cations are bonded to the four different ring nitrogen atoms of a xanthine^{3-} molecule [9].

We report here the structure of (xanthine$^+$)$_2$[ZnCl$_4$]. Some of the interest in investigating this compound originates from the possibility of documenting changes in bond angles and lengths within the xanthine molecule induced by protonation (or coordination) of ring nitrogen atoms.

Experimental

Synthesis

A solution of xanthine (300 mg, 1.97 mmol) and $ZnCl_2$ (3.0 g, 22.0 mmol) in 25 ml 3 N HCl was heated to boiling until complete solution of the ligand was observed. The hot reaction mixture was filtered and then kept for slow evaporation at 40 °C. After seven

*Author to whom correspondence should be addressed.

0020-1693/92/$5.00

days colorless transparent crystals could be isolated. In air, slight decomposition of the crystals was observed, indicated by opacity beginning at the surface. *Anal.* Calc. for $C_{10}H_{10}N_8O_4Cl_4Zn$: C, 23.39; H, 1.96; N, 21.82; Cl, 27.62. Found: C, 24.24; H, 2.09; N, 21.81; Cl, 26.19%.

Thermogravimetric data

The thermogravimetric data of the title compound, recorded on a Perkin-Elmer thermobalance TGS-2 are presented in Fig. 1. The thermal behaviour of (xanthine$^+$)$_2$[$ZnCl_4$], measured in flowing oxygen atmosphere is very similar to that described for the degradation of this compound in static air or nitrogen atmosphere [11]. The compound is stable up to about 300 °C. Its decomposition may be characterized as a one step overall reaction (complete dehalogenation followed by pyrolysis of xanthine) in the temperature range from 300 to 610 °C with two sharp increases in the reaction rate, as evidenced by two peaks in the derivative thermogravimetric curve at 360 and 400 °C. The diffraction data of the final product of the decomposition correspond with the values given for ZnO [12].

Crystallography

Owing to the observation of crystal deterioration upon standing in air, the single crystal of (xanthine$^+$)$_2$[$ZnCl_4$] had to be mounted in a glass capillary with inclusion of a drop of 2 N HCl solution. Cell parameters were determinated by least-squares refinement of 25 reflections in the interval $9 < \theta < 14°$. Intensity data were collected at room temperature on an Enraf-Nonius CAD-4 diffractometer. During data collection, the intensity of four standard reflections was monitored at an interval of every three hours to check crystal stability. A decrease of less than 1% was noted. To control the orientation of the crystal, four standard reflections were collected every 300 reflections. The intensities were corrected for Lorentz and polarization effects, and a numerical absorption correction on the basis of six crystal faces was applied. The structure was solved by Patterson syntheses using the program SHELXS86 [13]. Full-matrix least-squares refinement was carried out with SHELX76 [14] minimizing $\Sigma w(|F_o| - |F_c|)^2$, with $w = K/\sigma^2(F_o) + 0.00001F_o^2$ (K = 2.28). All five hydrogen atoms were found in the difference Fourier map and included in the least-squares refinements as a fixed contribution to F_c with thermal parameters assigned to $U = 0.04$ Å^2. The final refinements converged to $R = 0.042$ and $R_w = 0.040$. Maximum and minimum heights of the final difference Fourier map are 1.13 e Å^{-3} located 0.98 Å from Zn and -0.89 e Å^{-3} located 0.79 Å from Zn. Calculations were performed on a computer of the type HDS AS/XL V60. Crystal parameters, details of data collection and results of the refinement are summarized in Table 1. Refined atomic parameters and equivalent isotropic thermal parameters are listed in Table 2.

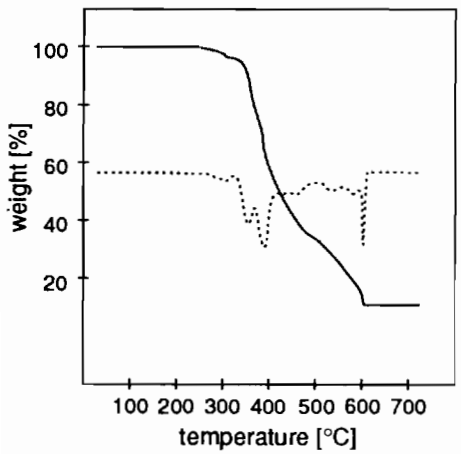

Fig. 1. Thermogravimetric degradation of (xanthine$^+$)$_2$[$ZnCl_4$]. Dotted lines represent derivative thermogravimetric curves.

Results and discussion

The compound (xanthine$^+$)$_2$[$ZnCl_4$] is built up from isolated [$ZnCl_4$]$^{2-}$ anions and two crystallographically equivalent non-coordinating xanthinium cations. The zinc ion and the chloride ions Cl(1) and Cl(2) are lying on the mirror plane perpendicular to the crystallographic *a* axis of the unit cell. The coordination tetrahedron of the zinc ion is completed by Cl(3) and its symmetry related chloride ion Cl(3′). The slightly distorted tetrahedral geometry with Zn–Cl distances ranging from 2.246(2) to 2.287(2) Å (mean value 2.272 Å) and Cl–Zn–Cl angles ranging from 105.1(1) to 113.0(1)° is characteristic for [$ZnCl_4$]$^{2-}$ ions. Corresponding mean Zn–Cl distances and ranges of tetrahedral angles are for example: 2.281 Å, 105.2–115.1° in (HDAMTP$^+$)[$ZnCl_4$] [15]; 2.269 Å, 104.7–113.6° in [Ru(en)$_3^{2+}$][$ZnCl_4$] [16]; 2.271 Å, 106.5–113.0° in (7-azaindolium$^+$)$_2$[$ZnCl_4$] [17]; 2.276 Å, 105.9–114.6° in (histaminium^{2+}) [$ZnCl_4$] [18]; 2.279 Å, 104.8–112.8° in (cytosinium$^+$)$_2$[$ZnCl_4$] [19]. Some distortion of the tetrahedral coordination geometry is always observed, but the extent of this distortion may depend on the specific N–H···Cl hydrogen bonding interaction of the [$ZnCl_4$]$^{2-}$ ions.

The xanthinium cations are approximately parallel to two faces of the [$ZnCl_4$]$^{2-}$ tetrahedron with the exocyclic oxygen atoms O(6) pointing between two chloride ions of these faces. In addition, the xanthinium ions are arranged in ribbons along the direction of the *b* and the *c* axes of the unit cell. The planes of the xanthinium cations are slightly tilted in respect to the

TABLE 1. Crystal data and structure determination parameters

Formula	$C_{10}H_{10}N_8O_4Cl_4Zn$
Formula weight	513.43
Crystal system	orthorhombic
Space group (No.)	$Pmn2_1$ (31)
a (Å)	19.701(6)
b (Å)	6.583(1)
c (Å)	6.610(2)
V (Å^3)	857.3(7)
Z	2
Calculated density (g cm^{-3})	1.99
Observed density (g cm^{-3})	1.98
Color, form	white, transparent, prismatic
Data crystal size (mm)	0.35×0.20×0.72
Absorption coefficient μ (cm^{-1})	19.9
Radiation (Å)	Mo Kα (λ=0.71073)
Minimum and maximum transmission coefficient	0.499–0.681
Data collection range, 2θ (°)	2–60
Range of h, k, l measured	−27, 0/−9, 9/−9, 9
Scan method	ω–2θ
Minimum and maximum scan speed (° min^{-1})	2.8, 5.5
Maximum counting time (s)	30
No. reflections measured (including standards)	5229
R_{av}/no. reflections averaged	0.047/4642
No. unique reflections	1284
Reflections with $I \geqslant 3\sigma(I)$	1129
No. variables	126
Largest shift/e.s.d. (non-hydrogen parameters)	0.001
Final maximum and minimum $\Delta\rho$ (e/Å^3)	1.13/−0.89
$R(F_o)$[a]	0.042
$R_w(F_o)$[b]	0.040

[a] $R = \Sigma||F_o| - |F_c||/\Sigma|F_o|$. [b] $R_w = [\Sigma w(|F_o| - |F_c|)^2/\Sigma w|F_o|^2]^{1/2}$.

TABLE 2. Atomic coordinates and equivalent isotropic or isotropic thermal parameters

Atom	x	y	z	U_{eq}/U_{iso}[a] (Å)
Zn	0.0000	0.1924(1)	0.0000	0.0250(2)
Cl(1)	0.0000	0.1900(4)	0.3459(3)	0.0360(6)
Cl(2)	0.0000	0.5223(3)	−0.0864(4)	0.0295(5)
Cl(3)	0.90677(8)	0.0224(2)	−0.1134(2)	0.0284(3)
N(1)	0.2070(2)	0.2528(6)	0.1837(9)	0.0248(11)
C(2)	0.2052(3)	0.1766(9)	0.3764(9)	0.0264(14)
O(2)	0.2277(2)	0.0091(7)	0.4168(7)	0.0400(11)
N(3)	0.1753(2)	0.2975(7)	0.5192(8)	0.0276(11)
C(4)	0.1473(3)	0.4761(9)	0.4602(9)	0.0241(13)
C(5)	0.1464(3)	0.5431(9)	0.2657(8)	0.0211(13)
C(6)	0.1790(3)	0.4297(9)	0.1096(9)	0.0217(13)
O(6)	0.1822(2)	0.4737(7)	−0.0713(6)	0.0299(10)
N(7)	0.1125(2)	0.7231(7)	0.2641(7)	0.0262(12)
C(8)	0.0923(3)	0.7639(10)	0.4479(10)	0.0347(16)
N(9)	0.1129(3)	0.6152(9)	0.5719(7)	0.0331(15)
H(1)	0.218	0.165	0.096	0.040
H(3)	0.164	0.258	0.648	0.040
H(7)	0.107	0.818	0.152	0.040
H(8)	0.071	0.882	0.503	0.040
H(9)	0.095	0.603	0.680	0.040

[a] $U_{eq} = \frac{1}{3}\Sigma_i\Sigma_j U_{ij} a^*_i a^*_j \mathbf{a}_i \cdot \mathbf{a}_j$.

(*bc*) plane. The molecular structure of the xanthinium cation with its thermal ellipsoids is presented in Fig. 2, and a stereo view of the unit cell is given in Fig. 3. Bonding distances and angles are summarized in Table 3.

The cations show a small but significant deviation from planarity in the pseudoaromatic ring system. Maximum deviations of an individual atom from the least-square plane through the nine ring atoms are 0.035 Å for C(2) and −0.025 Å for C(4). The extraannular

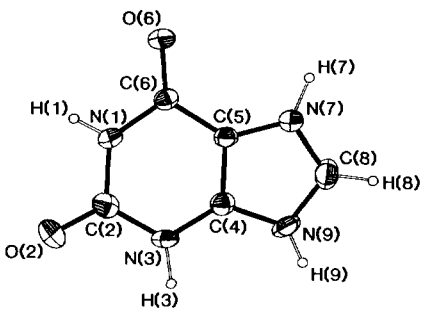

Fig. 2. ORTEP drawing of the xanthinium cation in (xanthine$^+$)$_2$[ZnCl$_4$] showing the atom labelling scheme. The thermal ellipsoids shown are drawn at the 50% probability level.

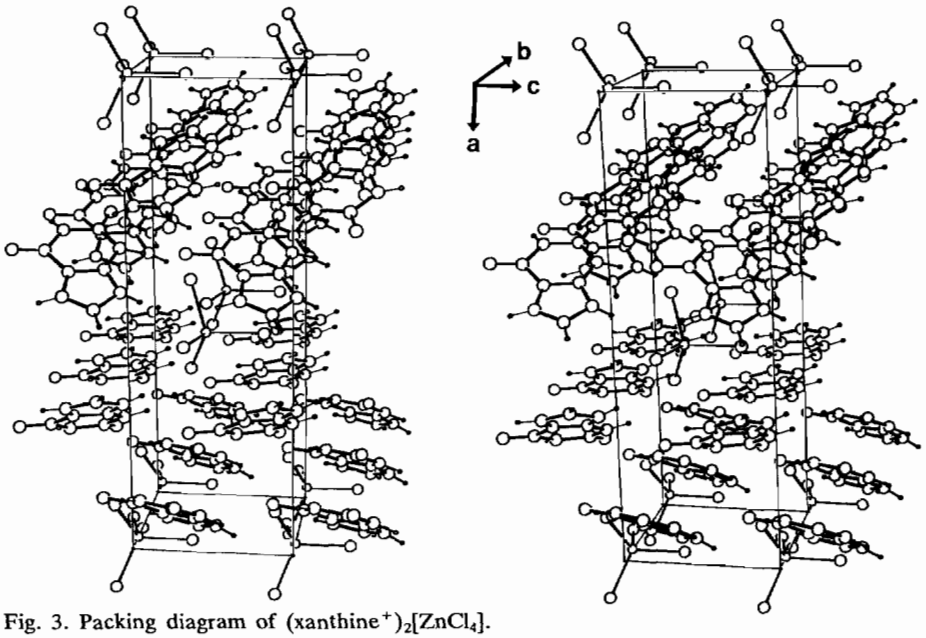

Fig. 3. Packing diagram of (xanthine$^+$)$_2$[ZnCl$_4$].

TABLE 3. Selected interatomic bond distances (Å) and angles (°) of (xanthine$^+$)$_2$[ZnCl$_4$]

Metal coordination polyhedron			
Zn–Cl(1)	2.287(2)	Zn–Cl(3)	2.277(2) (2×)
Zn–Cl(2)	2.246(2)		
Cl(1)–Zn–Cl(2)	105.1(1)	Cl(2)–Zn–Cl(3)	113.0(1) (2×)
Cl(1)–Zn–Cl(3)	109.0(1) (2×)	Cl(3)–Zn–Cl(3′)	107.5(1)
Xanthinium ion			
N(1)–C(2)	1.369(8)	C(5)–N(7)	1.360(8)
C(2)–N(3)	1.368(8)	N(7)–C(8)	1.306(8)
N(3)–C(4)	1.356(8)	C(8)–N(9)	1.340(8)
C(4)–C(5)	1.360(7)	N(9)–C(4)	1.357(8)
C(5)–C(6)	1.427(8)	C(2)–O(2)	1.219(7)
C(6)–N(1)	1.378(7)	C(6)–O(6)	1.232(6)
C(6)–N(1)–C(2)	129.0(6)	C(8)–N(9)–C(4)	108.1(5)
N(1)–C(2)–N(3)	116.1(5)	N(9)–C(4)–C(5)	106.8(5)
C(2)–N(3)–C(4)	118.7(5)	N(3)–C(4)–N(9)	129.2(6)
N(3)–C(4)–C(5)	124.0(6)	C(6)–C(5)–N(7)	132.2(5)
C(4)–C(5)–C(6)	120.5(5)	N(1)–C(2)–O(2)	121.7(6)
C(5)–C(6)–N(1)	111.4(5)	N(3)–C(2)–O(2)	122.2(6)
C(4)–C(5)–N(7)	107.3(5)	N(1)–C(6)–O(6)	121.6(6)
C(5)–N(7)–C(8)	108.8(5)	C(5)–C(6)–O(6)	127.0(6)
N(7)–C(8)–N(9)	109.0(6)		

oxygen atom O(2) lies 0.135 Å above this purine plane. This deviation probably also is a consequence of the strong hydrogen bonding interaction N(1)–H(1)···O(2). No significant deviation from the purine plane is observed for O(6).

Hydrogen atoms are bonded to all four ring nitrogen atoms of the xanthinium cation, thus inhibiting metal coordination at these sites. Therefore, in the salt-like structure of (xanthine$^+$)$_2$[ZnCl$_4$] the cations are only linked via an extended hydrogen bonding system to the [ZnCl$_4$]$^{2-}$ tetrahedra. A summary of bond distances and angles involving hydrogen bonding contacts is given in Table 4. Three N–H···Cl hydrogen bonds involving the hydrogen atoms H(3), H(7) and H(9) with donor–acceptor distances in the range 3.202(6)–3.434(6) Å are observed. In addition, the hydrogen atom H(3) participates in the hydrogen bond N(3)–H(3)···O(6), connecting translative equivalent xanthinium cations and leading to a bifurcated hydrogen bonding system around H(3). A strong hydrogen bonding interaction N(1)–H(1)···O(2) with a N···O distance of 2.782(7) Å occurs between two symmetry-related xanthinium cations.

TABLE 4. Hydrogen bonding contacts in (xanthine$^+$)$_2$[ZnCl$_4$]

X–H···Y	X–H (Å)	H···Y (Å)	X–Y (Å)	X–H···Y (°)
N(1)–H(1)···O(2)	0.841(5)	1.973(5)	2.782(7)	161.1(4)
N(3)–H(3)···O(6)	0.922(6)	2.364(5)	2.948(7)	121.1(3)
N(3)–H(3)···Cl(3)	0.922(6)	2.609(2)	3.434(6)	149.4(3)
N(7)–H(7)···Cl(3)	0.974(5)	2.229(2)	3.202(6)	177.3(3)
N(9)–H(9)···Cl(2)	0.802(5)	2.481(2)	3.229(6)	155.8(4)

Despite the pronounced layer-type structure of (xanthine$^+$)$_2$[ZnCl$_4$], no direct stacking interactions between the xanthinium cations are observed.

Most purine derivatives show significant alterations of the ring geometry resulting from hydrogen atom attachment at a nitrogen atom. Taylor and Kennard [20] have summarized the effects of protonation on the interatomic bond lengths and angles of nucleic acid constituents, using averaged geometries from numerous crystallographic data. In addition, such structural changes have also been elucidated from quantum chemical geometry optimizations at the semiempirical and *ab initio* level [21]. Generally, it can be stated that the changes of bond lengths and angles are more pronounced in the five-membered imidazole ring than in the six-membered pyrimidine ring. The major influence observed is an increase of about 3–4° of the C–N–C angle in the imidazole moiety upon protonation of the corresponding nitrogen atom compared with the respective neutral tautomer. Experimental data as well as our calculations show that this effect is accompanied by a reduction of approximately 3° of the adjacent angle N(7)–C(8)–N(9). In addition, a delocalization of the π-electron density between N(7)–C(8) and C(8)–N(9) has been observed upon simultaneous protonation of N(7) and N(9) for example in the purinium cations hypoxanthinium$^+$ [22] and 6-mercaptopurinium$^+$ [23]: the corresponding distances are shifted from 1.316/1.361 Å and 1.314/1.366 Å, respectively, in the neutral 1H,9H-tautomer to 1.325/1.330 Å and 1.333/1.340 Å, respectively, in the protonated 1H,7H,9H-tautomer, thus indicating a decrease of the double bond character of N(7)–C(8) and a corresponding increase of the double bond character of C(8)–N(9) upon protonation at N(7).

No crystal structure of free, neutral 1H,3H,7H-xanthine is known. Therefore, no detailed comparison of experimental bonding parameters of free, neutral xanthine with corresponding values of protonated xanthine is possible. Since however, three structure analyses of metal complexes involving N(9)-coordinating neutral 1H,3H,7H-xanthine have recently been reported [7], at least the influence of protonation in respect to metalation can be investigated by crystallographic data. The most significant alterations of the ring dimensions of the N(9)-protonated xanthinium cation, compared with an averaged experimental geometry involving N(9)-coordinating neutral xanthine, is an increase of 4.0° of the C(8)–N(9)–C(4) bonding angle. The experimental values are also indicative for a widening of the angle C(5)–N(7)–C(8) of 1.7° and a reduction of the N(7)–C(8)–N(9) angle of 3.6° upon protonation at N(9). In contrast to the significant alterations of the interatomic angles, and in contrast to the shifts of bond distances observed in hypoxanthine and in 6-mercaptopurine upon protonation at N(7), protonation of xanthine at N(9) induces only minor changes in the corresponding bonding distances. The bond length C(8)–N(9) remains practically unaffected, whereas the N(7)–C(8) bond even shows a small shortening in respect to the averaged distance in N(9)-coordinating xanthine, thus indicating a pronounced localization of the double bond between N(7) and C(8). These observed alterations of the bonding angles as well as the unexpected shifts of bond distances within the imidazole moiety of xanthine upon protonation are also supported by the results of quantumchemical calculations [21].

Supplementary material

Tables of anisotropic thermal parameters, hydrogen atom positions and listings of observed and calculated structure factors are available from the authors.

Acknowledgement

Research grants from the Swiss National Science Foundation (No 21-27924.89) are gratefully acknowledged.

References

1 L. G. Marzilli, *Prog. Inorg. Chem., 23* (1977) 255.
2 D. J. Hodgson, *Prog. Inorg. Chem., 23* (1977) 211.
3 E. I. Stiefel, *Prog. Inorg. Chem., 21* (1977) 1.
4 R. Hille and V. Massey, in T. G. Spiro (ed.), *Nucleic Acid Metal Interactions, Metal Ions in Biology 7,* Wiley, New York, 1985, p. 443.

5 J. B. Stanbury, J. B. Wyngaarden and D. S. Fredrickson (eds.), *The Metabolic Basis of Inherited Diseases*, Vol. 4, McGraw-Hill, New York, 1978.
6 A. Hesse and D. Bach, *Harnsteine, Klinische Chemie in Einzeldarstellungen*, Vol. 5, Georg Thieme, Stuttgart, 1982, p. 48.
7 E. Dubler, G. Hänggi and H. Schmalle, *Inorg. Chem.*, (1992) in press.
8 L. G. Marzilli, LA. Epps, T. Sorrell and T. J. Kistenmacher, *J. Am. Chem. Soc., 97* (1975) 3351.
9 F. Allaire and A. L. Beauchamp, *Can. J. Chem., 62* (1984) 2249.
10 A. L. Beauchamp, F. Bélanger-Gariépy, A. Mardhy and D. Cozak, *Inorg. Chim. Acta, 124* (1986) L23.
11 E. Colacio-Rodriguez, J. D. López-González and J. M. Salas-Peregrin, *J. Therm. Anal., 28* (1983) 3.
12 *Powder Diffraction File*, JCPDS, Swarthmore, PA, Cards No. 36-1451.
13 G. M. Sheldrick, SHELXS86, in G. M. Sheldrick, C. Krüger and R. Goddard (eds.), *Crystallographic Computing*, Oxford University Press, Oxford, 1985, p. 175.
14 G. M. Sheldrick, *SHELX76*, program for crystal structure determination, University of Cambridge, UK, 1976.
15 M. A. Romero, J. M. Salas, R. López, M. D. Gutiérrez, K. Panneerselvam, K. K. Chacko, K. Aoki and H. Yamazaki, *Inorg. Chim. Acta, 172* (1990) 253.
16 P. J. Smolenaers, J. K. Beattie and N. D. Hutchinson, *Inorg. Chem., 20* (1981) 2202.
17 W. S. Sheldrick, *Z. Naturforsch., Teil B, 37* (1982) 653.
18 L. B. Cole and E. M. Holt, *Acta Crystallogr., Sect. C, 46* (1990) 1737.
19 P. E. Bourne and M. R. Taylor, *Acta Crystallogr., Sect. C, 39* (1983) 430.
20 R. Taylor and O. Kennard, *J. Mol. Struct., 78* (1982) 1.
21 G. Hänggi, *Ph.D. Dissertation*, University of Zürich, Switzerland, 1991.
22 H. Schmalle, G. Hänggi and E. Dubler, *Acta Crystallogr., Sect. C, 46* (1990) 340.
23 E. Dubler and E. Gyr, *Inorg. Chem., 27* (1988) 1466.